Journal of Materials Chemistry B

Accepted Manuscript

ROYAL SOCIETY OF CHEMISTRY

www.rsc.org/materialsB

Antioxidant nanozyme: A facile synthesis and evaluation of reactive oxygen species scavenging potential of nanoceria encapsulated albumin nanoparticles

Bharat Bhushan[1], P.Gopinath[1,2] *

Nanobiotechnology Laboratory,

[1]Centre for Nanotechnology, Indian Institute of Technology Roorkee,

[2]Department of Biotechnology, Indian Institute of Technology Roorkee,

Roorkee, Uttarakhand-247667, India.

*Corresponding author: Tel. +91-1332-285650; Fax. +91-1332-273560;

E-mail: pgopifnt@iitr.ernet.in, genegopi@gmail.com

Abstract

Several diseases and disorders including cancer are endorsed by the excessive oxidative stress caused due to incomplete removal of reactive oxygen species (ROS) by the antioxidant defense system of the body. Therefore present interest among the scientific community lies in the development of highly stable, biocompatible artificial enzymatic system that possesses a high ROS scavenging activity over a period of time. In recent years catalytic nanoparticles emerged as a potential candidate in the field of nanomedicine. Due to their inherent catalytic properties they are exploited as an artificial enzyme (nanozyme), to reinstate or correct aberrant enzymatic activities in patients. Among them cerium oxide nanoparticles/nanoceria (CNPs) emerged as a potent artificial redox enzyme, mimicking the activity of superoxide dismutase (SOD) and catalase and endure a tremendous ROS scavenging potential as depicted in a surfeit of human cell lines and animal models. In the present article, a facile synthesis of biocompatible nanoceria encapsulated albumin nanoparticles (BCNPs) *via* desolvation technique that lead to the abatement of intracellular ROS is reported. Physico-chemical characterizations of as-prepared BCNPs corroborate the formation of highly monodispersed, spherical and aqueous stable delivery system. Interestingly, such entrapment does not affect the enzyme mimetic activity of CNPs as demonstrated by SOD assay. The biocompatibility and ROS scavenging potential of BCNPs were further assessed *in vitro* against human lung epithelial cells by cell viability assay and flow cytometric analysis, respectively. The quantitative and qualitative assessments of cellular uptake of BCNPs were done by inductively coupled plasma mass spectrometry (ICP-MS), transmission electron microscope (TEM) and field emission scanning electron microscope (FE-SEM) analysis. Furthermore, the BCNPs preserve the cell's antioxidant defense system and

protect them from oxidant-mediated apoptosis as confirmed by semi-quantitative RT-PCR analysis. Thus, the as-prepared BCNPs could provide an opportunity to be utilized as a potential candidate against ROS induced diseases and disorders.

KEYWORDS

Albumin nanoparticles, nanoceria, reactive oxygen species, oxidative stress, antioxidant, nanozyme

Introduction

ROS generated as a byproduct due to the incomplete reduction of oxygen in aerobic metabolism, which could be involved in cell signaling including induction of apoptosis and protection against pathogen. However, the excess level of ROS in the body leads to cell damage that endorse a variety of disorders and diseases such as Alzheimer, Parkinson, cardiovascular dysfunctions, inflammatory conditions, aging and cancer [1-4]. Antioxidant enzymes mainly SOD, catalase, and glutathione peroxidase are generated by the cells in response to defend the body from detrimental effects of ROS [5]. However, in case of sudden oxidative damage such enzymes are found to be insufficient to protect the cells. This provokes a need to develop an artificial antioxidant enzyme mimetic system that has high ROS scavenging potential, biocompatible, maintains stability inside the cells and provide high therapeutic index.

In the recent years, metal based nanoparticles have shown their tremendous potential for biomedical applications. In particular, gold, silver, silica and iron oxide based nanoparticles are

widely used for cancer therapeutic and bio-imaging applications [6]. In this plethora of nanomaterials, CNPs emerged as a potential candidate due to its SOD and catalase mimetic activity, high biocompatibility and auto-regenerative properties. The CNPs act as a catalyst having a mixed valency, exists in either reduced (+3) or oxidized (+4) state. As reported earlier CNPs in (+3) state found to have SOD mimetic activity thereby catalyzes the superoxide radical anion dismutation in living cells [7-9], while in (+ 4) state demonstrate catalase mimetic activity with the capability to decompose H_2O_2 to O_2 and H_2O [7,10]. The antioxidant potential of CNPs has been well demonstrated in protecting the cells from ROS as revealed in a surfeit of cell culture and animal models [11-14]. However, the short residence time in body, poor solubility and use of harmful solvents during the synthesis remains unresolved challenges that hamper their potential biomedical applications. This provokes a need to explore a potential delivery system for CNPs in order to promote its biomedical applications.

Inherent properties of protein based delivery system including availability, lack of toxicity and immunogenicity, preferential cellular uptake, biocompatibility, ease of chemical modification and biodegradability provided them an edge over other available delivery system [6, 15-16]. Albumin nanoparticles based delivery systems have gained tremendous interest in the field of biomedical applications. A number of albumin based drug nanoformulation have been designed so far, which are available in market and under clinical trial. Among them the most admired one was food and drug administration (FDA) approved Abraxane (a paclitaxel loaded albumin nanoparticles) designed for the treatment of metastatic breast cancer and advanced non-small-cell lung cancer [17-19]. This augmented the interest in utilizing albumin nanocarrier to develop an artificial antioxidant mimetic enzyme loaded delivery system. Such artificial enzyme remain

stable inside the cells and provide desired steady state level of therapeutic dose as a result of controlled release of CNPs that helps in defending the cells against actively generating ROS over a period of time. The current study demonstrated a feasible and highly reproducible method to form CNPs encapsulated albumin nanoparticles (BCNPs) without altering their antioxidant activity. Such delivery system was further typified and examined *in vitro* for their role in protection against ROS in human lung epithelial cell line (L-132). Moreover, the as-prepared BCNPs were also assessed for their biocompatibility and cellular uptake by L-132 cells.

Results and discussion

Encapsulation of CNPs in albumin nanoparticles

CNPs were prepared by the hydrothermal method as described earlier [20]. The prepared CNPs were evaluated by UV-visible spectrophotometer showing a characteristic broad absorption peak around 330 nm as shown in Fig. S1. Fig. S2 (a) indicates the TEM micrograph of the as-prepared CNPs. The TEM image implies that the average size of the uniformly distributed prepared CNPs is 4.35 ± 1.07 nm as shown in Fig. S2 (b) and Fig. S2 (c) depict the corresponding EDX pattern. The prepared CNPs were encapsulated inside the albumin nanoparticles *via* desolvation technique [21], using ethanol as desolvating agent and glutaraldehyde as cross linking agent as shown in Fig. 1. The bifunctional reagent glutaraldehyde endorses to the creation of Schiff bases among the two carbonyl groups of glutaraldehyde and the positively charged amino groups of protein resulted in the formation of least aggregated spherical BCNPs with uniform distribution.

Characterizations: Surface morphology and particle size

The surface morphology of the prepared BCNPs was determined by FE-SEM as shown in Fig. 2 (a). The FE-SEM micrograph of BCNPs depicts a spherical morphology with uniform size distribution. Moreover, the TEM image of BCNPs as shown in Fig. 2 (c), clearly illustrated the distribution of CNPs inside the albumin nanoparticles, which confirmed the formation of CNPs encapsulated albumin nanoparticles.

The particle size distribution of prepared BCNPs was obtained by using dynamic light scattering (DLS) as shown in Fig. 2 (d). The average hydrodynamic size of the prepared BCNPs was found to be 278.4 nm. Further, the size of the BCNPs was also analyzed by atomic force microscopy (AFM) as shown in Fig. 2 (b). The average grain size of BCNPs was found to be 231.05 nm after processing the image through NOVA software. The size of the prepared nanoparticles lies within the optimal range comparable to the already prepared albumin based nanoparticles.

X-ray diffraction (XRD) analysis

Physical nature of the prepared BCNPs was assessed by XRD analysis. Fig. 3 (a) showed the XRD pattern of CNPs and BCNPs. The prepared CNPs have a cubic, fluorite type structure showing a characteristic diffraction peaks at 28.5, 33.1, 47.4 and 56.3 corresponding to 111, 200, 220, 311 crystal planes that resembled with CeO_2 (JCPDS 78-0694). However, no such peaks were observed in case of BCNPs depicting the encapsulation of CNPs and no significant amount of CNPs were left in the system after interaction with protein. On comparing the prepared

BCNPs with free CNPs, BCNPs were found to be more amorphous in nature, which might be due to the cross linking mechanism happening between the reactive functional groups of protein and CNPs along with the prominent electrostatic interaction between them may perhaps ascribe to the amorphous nature of the BCNPs. [22]

Fourier transform infrared spectroscopic (FTIR) analysis

Surface chemistry of the nanoparticles play crucial role in their interaction with protein. Several factors including hydrophobic interactions, electrostatic interaction and chemical interaction are among the leading factor responsible for protein-nanoparticle complex formation. As reported earlier electrostatic interaction was the major factor responsible for the CNPs interaction with BSA. Moreover, higher the positive zeta potential more will be the interaction. As in our case CNPs also have high value of zeta potential around 36.3 mV, while BSA have net negative charge in water (pH=7), suggesting that electrostatic interaction are mainly responsible for CNPs interaction with BSA [23-24].

In Fig. 3 (b) major peaks were observed around 1652, 1540, 3070 and 3420 cm^{-1} for pristine BSA corresponding to the amide I (C=O stretching vibration), amide II (N–H bending vibration and C-N stretching vibration), amide A (-NH stretching vibration) and –OH stretching vibration respectively, as discussed previously [21]. While the FTIR spectrum of CNPs showing major characteristic peaks are listed in Table S1. Peaks around 3431.12, 1630.32 corresponded to the physically adsorbed water on the surface of the CNPs, while the major peak around 439.51 corresponding to the Ce-O stretching band confirms the formation of CNPs [25-26]. The

absorption peak around 2925.38 cm^{-1}could be assigned to a stretching vibration of the C-H group. Moreover, a strong peaks were observed at 1538.41 and 1455.76 corresponds to the symmetric and asymmetric stretching vibration of carboxylic group of acetic acid. The spectra suggests that carboxyl group of acetic acid get chemically bound to the surface of synthesized CNPs imparting them high colloidal stability and zeta potential [26-30]. The chemical species on surfaces of CNPs were further indentified by thermo gravimetric (TG) analysis of CNPs depicting a slight weight loss in the temperature range between 25 and 900 ^{o}C. In Fig. S3 up to 200 ^{o}C slight weight loss was observed which corresponds to the desorption of the adsorbed water but beyond 200 ^{o}C a sudden loss in weight was observed as a result of carboxyl groups on the surface of CNPs confirming the FTIR outcomes [25].

On comparing the IR spectra of CNPs, BSA alone and BCNPs as shown in Fig. 3(b), a major shift in the peaks were observed from 3431.12 to 3298.27, 1455.76 to 1448.92 suggesting the involvement of –OH and C=O groups of CNPs in their interaction with protein. Moreover, in case of BCNPs, a characteristic suppression in the stretching frequency was observed and the peaks were appeared as a wide spectrum on account of possible interaction between the nanoparticles. A slight shift in the amide I, amide II and amide III peaks were observed, which may be attributed to the cross-linking mechanism amongst the protein amino groups and the possible interaction of protein with CNPs. [22, 31-32].

Thermal stability of the nanoparticles

TG analysis was conducted for BCNPs and pristine BSA (control), results demonstrated the slower rate of degradation for BCNPs as compared to pristine BSA suggesting the enhanced stability of BCNPs. Fig. 3 (c) clearly depicts that degradation of pristine BSA start from 200^{o}C but no such change was observed for BCNPs. However, beyond 250^{o}C, a sudden weight loss was observed for both particles which could be due to the loss of small molecules such as ammonia, CO_2 etc. At 400-450^{o}C a substantial distinction in weight loss was observed, as 24% was left for control BSA whereas 42% was remained for BCNPs which validate the slower degradation rate for BCNPs as compared to BSA alone. Beyond 450 ^{o}C, degradation rate of BCNPs became faster as compared to pristine BSA, which could be attributed to the crystalline nature of encapsulated CNPs in BCNPs. While, no noteworthy change was detected in BSA (control) owing to the char formation in nitrogen atmosphere as recently reported. [33]

***In Vitro* Stability of BCNPs**

Stability of the carrier molecule always play a crucial role for their future clinical applications, as the cargo molecules slowly escape from the carrier and form secondary aggregates that might leads to severe complications. Further, the higher stability is also correlated with the long circulation time *in vivo* and sustained release of cargo molecules. To evaluate the physiological stability of BCNPs in aqueous and PBS (pH= 7.4) solutions, the variation in particle size distribution of BCNPs were examined by DLS *in vitro* for more than 96 h. As shown in Fig.3 (d), in aqueous and PBS solution mean particle size of the BCNPs remain constant for 96 h at

25^{o}C. Thus, confirmed the higher stability of BCNPs under *in vitro* physiological conditions supporting their future clinical applications.

Encapsulation efficiency of nanoparticles

A range of concentrations of the CNPs with albumin nanoparticles were taken and the BCNPs were prepared *via* desolvation technique. The encapsulation efficiency of the albumin nanoparticles was examined by using various concentrations of CNPs, whilst the carrier concentration was remains same. The protein-CNPs complex with the paramount encapsulation efficiency was opted for remaining studies. As shown in Fig. 4(a), 5:25 ratio of CNPs: BSA provides the maximum encapsulation efficiency of 82.34%.

***In vitro* release study**

The *in vitro* release kinetic pattern of CNPs from BCNPs was studied for over 96 hours at pre defined time intervals in PBS at pH 7.4 as shown in Fig. 4(b). The *in vitro* release is a combined outcome of diffusion of nanoparticles out of the nanocarrier into the exterior environment and simultaneous degradation of carrier molecules. A biphasic release kinetic pattern was found having an initial burst release of 31.79% in the first 10 hours followed by a controlled release of the CNPs. The initial burst release was attributed to the simultaneous release of the surface bound CNPs and encapsulated CNPs from the BCNPs, whereas the later sustained release was correspond to the encapsulated CNPs. In the following 24 hours, the cumulative release reached 40.88% in a sustained manner, making albumin nanoparticles as a potential nanoplatform for the

sustained release of CNPs in order to protect the cells from ROS over a period of time. It is noteworthy that as expected the overall release of CNPs from BCNPs was found to be slower unlike the release profile of other encapsulated drugs in the albumin nanoparticles, which might be due to the limited solubility of oxide nanoparticles.

Moreover, the improved stability of BCNPs and their sustained release profile in the physiological buffer was attributed to the glutaraldehyde mediated cross linking mechanism of protein nanoparticles. The results suggested that the sustained release of CNPs from BCNPs in the media not only protect the cells from sudden exposure to higher concentration of CNPs but also help in fighting against the intracellular ROS for a considerable period of time making albumin nanoparticles a better delivery system for future applications in the field of nanomedicine.

SOD activity of CNPs

The SOD mimetic activity of released CNPs from BCNPs was examined as shown in Fig. 5. A time dependent increase in the SOD mimetic activity of the CNPs was observed which correlates with the increase in the concentration of CNPs in the surrounding medium as a result of its release from the BCNPs. During the first 10 h, due to the initial burst release of CNPs from BCNPs a significant increment in the SOD activity was observed as a result of higher concentration of CNPs in the surrounding medium. While a steady increment in the SOD activity was observed from 24 to 96 h due to the sustained release of CNPs from the BCNPs. Thus the retention of antioxidant potential of released CNPs ensures that the BCNPs can be used for further therapeutic applications.

Cell viability assay

The cytotoxicity of CNPs, BCNPs and nanocarrier (i.e. BSA NPs) were evaluated quantitatively on the L-132 cells by MTT dye reduction method as shown in the Fig. 6 and Fig. S4. The results demonstrated that alike BSA NPs, alone CNPs and BCNPs were found to be non-toxic to L-132 cells up to a concentration of 300 μg mL^{-1}. More than 80% cell viability was observed after 24 hours confirming the biocompatibility of CNPs, BCNPs and non-toxic nature of bare BSA nanoparticles.

Cellular uptake studies

Cellular uptake play a crucial role in the development of successful nanocarrier platform as it contributes to the uptake of the cargo molecule by the cells and their sustained release from the nanocarrier. In the present study, the uptake of CNPs encapsulated albumin nanoparticles was investigated *invitro* by incubating the L-132 cells with BCNPs and then followed by their qualitative analysis by FE-SEM, TEM and quantitative analysis by ICP-MS. The FE-SEM images of L-132 cells treated with BCNPs (Fig. 7 (c)) clearly demonstrated that the treatment of cells with BCNPs did not affect the cells as showed by the healthy morphology of the cells. Moreover, the encapsulation of CNPs in albumin enhanced the biological acceptability of the nanoparticles. The BCNPs get easily attached on the surface of the cells as indicated by the arrows in Fig. 7 (c) and gets internalized by the cells as highlighted in the box. The elemental mapping of the highlighted area as shown in Fig. 7(d) clearly depicts the defined distribution profiles of elements Ce (red color corresponds to CNPs), N (nitrogen) and C (carbon) (N and C

denoted by yellow and green color, respectively). Moreover, the EDX analysis of highlighted area further confirms the study as shown in Fig. S5. Thus, the results clearly signify the uptake of BCNPs by the cells.

The TEM image of treated L-132 cells showed healthy morphology, while the arrow indicates the successful delivery of CNPs inside the cells by the albumin nanocarriers as showed in Fig. 7 (a). The EDX analysis as showed in Fig. S5 further confirmed the presence of CNPs within the cells.

Moreover, ICP-MS analysis conducted to quantify the cellular uptake of CNPs in L-132 cells treated with BCNPs for different time interval. The results demonstrated that the cellular uptake of CNPs was found to be increased in a time dependent manner as showed in Fig.7 (b), which further confirmed the potential uptake of the CNPs encapsulated albumin nanoparticles and the sustained release of CNPs from it.

ROS scavenging potential of BCNPs

The ROS scavenging potential of BCNPs was assessed in L-132 cells exposed to H_2O_2 mediated oxidative stress and ROS generation. As depicted in Fig. S7, no considerable changes in the level of ROS production took place on incubating the cells with BCNPs for different time interval as compared to untreated control. The results suggested that the BCNPs did not endorse ROS generation. In spite of that a major decrease in the DCF fluorescence intensity corresponding to the ROS content was observed when L-132 cells were exposed to H_2O_2, after preincubating the cells with BCNPs for different time intervals. As shown in Fig. 8, a time dependent decrease in the level of ROS generation was observed as a result of sustained release of the CNPs from the

BCNPs in combination with the increased intracellular level of CNPs. Initially, a significant intracellular ROS generation was detected as a result of low intracellular concentration of CNPs but with the increase in the duration of incubation significant amount of CNPs gets internalized in the cells that lead to the reduction in the intracellular ROS level, when L-132 cells were challenged to H_2O_2. In case of L-132 cells preincubated with BCNPs for 96 h, a fivefold decrease in the intracellular ROS production was observed as compared to BCNPs untreated cells. Similarly, on pre-incubating the cells with different concentration of free nanoceria depicts a concentration dependent ROS scavenging property of CNPs as shown in Fig. S8. Initial low concentration of CNPs was found to be ineffective and high concentrations of free CNPs were required for effective intracellular ROS abatement. The inadequate intracellular ROS scavenging potential of free nanoceria might be correlated with the high positive zeta potential value of CNPs. As reported in previous literature [23], higher the positive zeta potential of the CNPs lower will be the cellular uptake. The encapsulation of CNPs inside the albumin nanoparticles enhanced the cellular uptake of CNPs and thereby augmented the therapeutic efficacy of CNPs. Such abatement of intracellular ROS was also confirmed by corresponding fluorescent images of L-132 cells preincubated with BCNPs for different time period as shown in Fig. 8 (b). In H_2O_2 treated cells strong fluorescence was observed due to high level of ROS production as compared to BCNPs and H_2O_2 untreated cells. Moreover, the fluorescent signal of BCNPs pretreated L-132 cells decrease with increase in BCNPs pre-incubation time suggesting an efficient removal of ROS. Thus the present study clearly revealed that the uptaken BCNPs are effective antioxidant agent and BCNPs pretreatment significantly attenuates ROS production over a period of time comparable to the H_2O_2 untreated cells. Moreover, long term ROS scavenging action of CNPs, suggests their unprecedented role for future conventional antioxidant drugs.

Gene expression studies

The antioxidant potential of CNPs encapsulated BSA NPs was assessed *in vitro* in L-132 cells *via* semi-quantitative RT-PCR analysis. The gene expression studies implied that BCNPs effectively defend the cells against oxidative stress and prevent the cells from entering into oxidative stress induced apoptosis as shown in Fig. 9. In all such experiments the expression of housekeeping gene GAPDH was taken as internal control, which remains unchanged during the process.

Oxidative stress arises as results of overproduction of ROS or incomplete removal of ROS because of decrease in the antioxidant levels. Antioxidant enzymes protect the cells from oxidative stress by comprising the primary defense system. Among them catalase, glutathione peroxidase and SOD are major enzymes, which are present in all the cells and plays a decisive role to fight against the H_2O_2 and the superoxide radical induced oxidative stress, respectively, and thereby maintain the integrity of the cell membrane.[34-35]. It was observed that the activity of antioxidant enzymes including catalase, glutathione peroxidase and SOD was found to be down regulated when L-132 cells were exposed to H_2O_2 as compared to the control. Such perturbation makes the cells more vulnerable to oxidative damage. However, no changes were found in the level of gene expression in case of BCNPs treated cells. But when the cells pre-incubated with BCNPs got exposed to H_2O_2, the level of antioxidant enzymes was found to be higher as compared to H_2O_2 treated cells. The increase in the level of gene expression in case of BCNPs preincubated cells may be correlated with the ROS scavenging activity of the BCNPs. Thus the present results confirm the antioxidant potential of the BCNPs and are supported by previous studies [36-38].

Moreover, BCNPs also protect the cells from entering the oxidative stress induced apoptosis. The exposure of cells with H_2O_2 leads to the induction of apoptotic gene expression. An increase in the expression of caspase-3, a major factor that is responsible for initiation and execution of apoptosis [39] was observed in H_2O_2 treated cells. In case of BCNPs treatment the level of caspase-3 was down-regulated which suggest that the antioxidant property of BCNPs helps in protecting the cells by removing the free radicals. Similarly, the level of anti-apoptotic gene (e.g. basal cell lymphoma-extra large (Bcl-xl)) [40] was found to be down regulated in H_2O_2 treated cells, while an increase in the level of expression was observed on BCNPs pretreatment before the addition of hydrogen peroxide.

Conclusion

In the present study, a novel artificial antioxidant encapsulated delivery system based on biodegradable albumin nanoparticles was developed. Alike any other drugs CNPs were encapsulated inside BSA NPs using desolvation method. The delivery and sustained release of CNPs *via* biocompatible protein nanocarriers had not been addressed so far with this perspective. The physicochemical characterization of as-prepared BCNPs were done by AFM, FE-SEM and DLS depicting that even after CNPs entrapment the size of BCNPs lies within optimal range required for drug delivery applications. The MTT results revealed the biocompatibility of BNPs and BCNPs. Further, SOD and flow cytometric analysis revealed that the encapsulation of CNPs did not alter its antioxidant activity essential for their therapeutic applications. The cellular uptake studies of BCNPs conducted via TEM, FESEM and ICP-MS in L-132 cells depicted considerable internalization of CNPs inside the cells, implying the usefulness of these NPs for therapeutic applications. Gene expression analysis demonstrated the successful defense of cells

against free radical and oxidative insults. Thus our studies propose that the therapeutic potential of CNPs could be better utilized by encapsulating it in biocompatible protein based nanocarrier for various biomedical applications.

Acknowledgements

This work was supported by the Indian Council of Medical Research, Science and Engineering Research Board (No.SR/FT/LS-57/2012) and Department of Biotechnology (No.BT/PR6804/GBD/27/486/2012), Government of India. BB is thankful to the Ministry of Human Resource Development, Government of India, for the fellowship. Sincere thanks to Department of Chemistry and Institute Instrumentation Centre, IIT Roorkee for the various analytical facilities provided.

References

1. B. Kumar, S. Koul, L. Khandrika, R. B. Meacham and H. K. Koul, *Cancer Res*., 2008, **68**, 1777–1785.
2. J. Emerit, A. Edeas and F. Bricaire, *Biomed. Pharmacother*., 2004, **58**, 39–46.
3. M. K. Misra, M. Sarwat, P. Bhakuni, R. Tuteja and N. Tuteja, *Med. Sci. Monit*., 2009, **15**, 209–219. 21.
4. T. Finkel and N. J. Holbrook, *Nature*., 2000, **408**, 239–247.
5. E. D. Harris, *J. FASEB*., 1992, **6**, 2675-2683.
6. U. K. Sukumar, B. Bhushan, P. Dubey, I. Matai, A. Sachdev and P. Gopinath, *Int. Nano Lett.*, 2013, **3**, 45–53.

7. C. Korsvik, S. Patil, S. Seal and W. T. Self, *Chem. Commun*., 2007, **10**, 1056–1058.
8. A. S. Karakoti, N. A. Monteiro-Riviere, R. Aggarwal, J. P. Davis, R. J. Narayan, W. T. Self, J. McGinnis and S. Seal, *JOM.*, 2008, **60**, 33–37.
9. E. G. Heckert, A. S. Karakoti, S. Seal and W. T. Self, *Biomaterials*., 2008, **29**, 2705–2709.
10. T. Pirmohamed, J. M. Dowding, S. Singh, B. Wasserman, E. Heckert, A. S. Karakoti, J. E. King, S. Seal, and W. T. Self, *Chem. Commun*., 2010, **46**, 2736–2738.
11. J. McGinnis, S. Patil, L. Wong, S. Sezate, J. Chen and S. Seal, US Pat., 7727559, 2010.
12. R. W. Tarnuzzer, J. Colon, S. Patil and S. Seal, *Nano Lett*., 2005, **5**, 2573–2577.
13. G. A. Silva, *Nat. Nanotechnol*., 2006, **1**, 92–94.
14. I. Celardo, J. Z. Pedersen, E. Traversa and L. Ghibelli, *Nanoscale*., 2011, **3**, 1411–1420.
15. B. Bhushan, U. K. Sukumar, I. Matai, A. Sachdev, P. Dubey and P. Gopinath, *J. Biomed. Nanotechnol*., 2014, **10**, 2950–2976.
16. P. Gopinath, S. Uday Kumar, I. Matai, B. Bhushan, D. Malwal, A. Sachdev and P. Dubey, Cancer Nanotheranostics., *Springer briefs in applied science and technology* ., 2015, 1-93.
17. N. K. Ibrahim, N. Desai, S. Legha, P. Soon-Shiong, R. L. Theriault,E. Rivera, B. Esmaeli, S. E. Ring, A. Bedikian, G. N. Hortobagyi and J. A. Ellerhorst, *Clin. Cancer Res*., 2002, **8**, 1038–1044.
18. E. Miele, G. P. Spinelli, E. Miele, F. Tomao and S. Tomao, *Int. J. Nanomedicine.*, 2009, **4**, 99–105.
19. M. R. Green, G. M. Manikhas, S. Orlov, B. Afanasyev and A. M. Makhson, *Ann. Oncol*., 2006, **17**, 1263–1268.

20. X. Y. Liu, W. Wei, Q. Yuan, X. Zhang, N. Li, Y. G. Du, G. H. Ma, C. H. Yan and D. Ma, *Chem. Commun.*, 2012, **48**, 3155–3157.

21. B. Bhushan, P. Dubey, S. Uday Kumar, A. Sachdev, I. Matai and P. Gopinath, *RSC Adv*., 2015, **5**,1 2078–12086.

22. N. S. Rejinold, M. Muthunarayanan, K.P. Chennazhi, S.V. Nair and R. Jayakumar, *J. Biomed. Nanotech.*, 2011, **7**, 521-534.

23. S. Patil, A. Sandberg, E. Heckert, W. Self and S. Seal, *Biomaterials*, 2007, **28**, 4600–4607.

24. D. Yuan, Z. Shen, R. Liu, Z. Chi and J. Zhu, *J. Biochem. Mol. Toxicol*., 2011, **4**, 263-268.

25. X. Jiao, H. J. Song, H. H. Zhao, W. Bai, L. C. Zhang and Y. Lv, *Anal. Methods.*, 2012, **4**, 3261–3267.

26. E. Kumar, P. Selvarajan and D. Muthuraj, *Mater. Res*., 2013, **16**, 269-276.

27. S. K. Pahari, N. Sutradhar, A. Sinhamahapatra, P. Pal and A. B. Panda, *New J. Chem.*, 2011, **35**, 1460-1465.

28. T. Masui, H. Hirai, N. Imanaka, G. Adachi, T. Sakata and H. Mori, *J. Mater. Sci. Lett.*, 2002, **21**, 489–491.

29. E. K. Goharshadi, S. Samiee and P. Nancarrow, *J. Colloid Interface Sci*., 2011, **356**, 473−480.

30. D. Girija, H. S. B. Naik, C. N. Sudhamani and B. V. Kumar, *Arch. Appl. Sci. Res.*, 2011, **3**, 373–382.

31. J. Kong and Y. U. Shaoning, *Acta. Biochimica. et Biophysica. Sinica.*, 2007, **39**, 549–559.

32. P. Huang, Z. Li, H. Hu and D. Cui, *J. Nanomater.*, 2010, **2010**, 641545.

33. A. Gebregeorgis, C. Bhan, O. Wilson and D. Raghavan, *J. Colloid Interface Sci.*, 2013, **389**, 31–41.

34. T. Ando, K. Mimura, C. C. Johansson, M. G. Hanson, D. Mougiakakos, C. Larsson, T. Martins da Palma, D. Sakurai, H. Norell, M. Li, M. I. Nishimura and R. Kiessling, *J. Immunol.*, 2008, **181**, 8382.

35. B. Halliwell and J. M. C. Gutteridge, *Drugs Aging*., 2001, **18**, 685–716.

36. J. Niu, K. Wang and P. E. Kolattukudy, *J. Pharmacol. Exp. Ther.*, 2011, **338**, 53–61.

37. M. D. Pandareesh, T. Anand and P. V. Bhat, *Cytotechnology*., 2014, doi 10.1007/s10616-014-9767-3.

38. G. Zhou, Y. Li, B. Zheng, W.Wang, J. Gao, H. Wei, S. Li, S.Wang and J. Zhang, *Micro. Nano. Lett*., 2014, **9**, 91-96.

39. S. L. Fink and B. T. Cookson, *Infect. Immun.*, 2005, **73**, 1907-1916.

40. R. S. Y. Wong, *J. Exp. Clin. Cancer Res.*, 2011, **30**, 87.

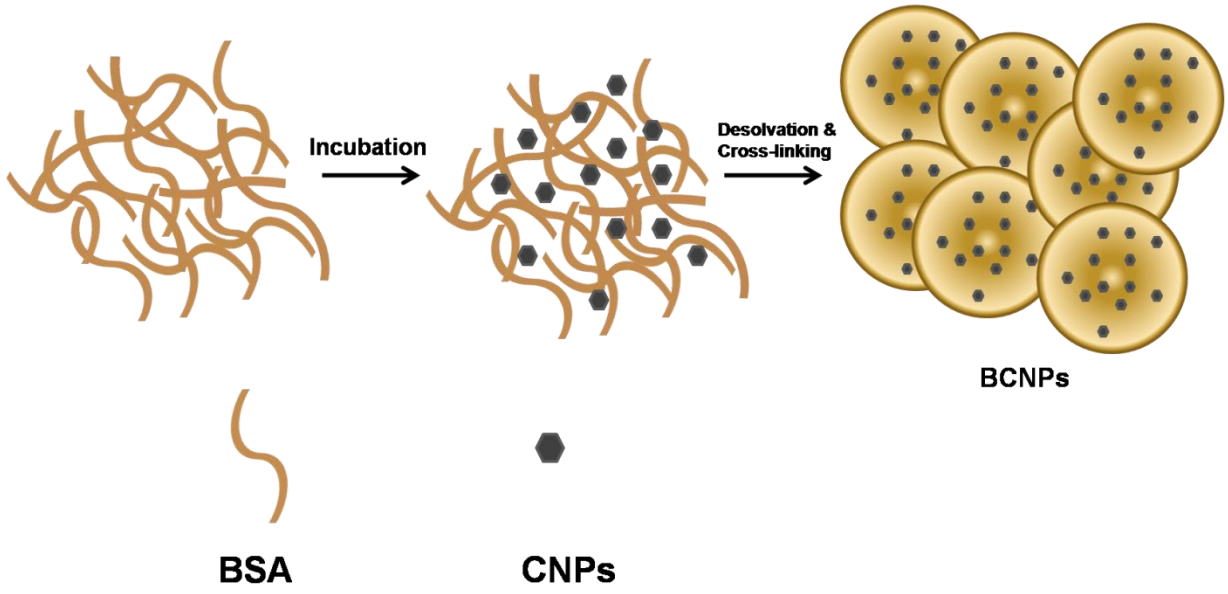

Fig. 1 Schematic outline of nanoceria encapsulated albumin NPs (BCNPs) fabrication by desolvation technique

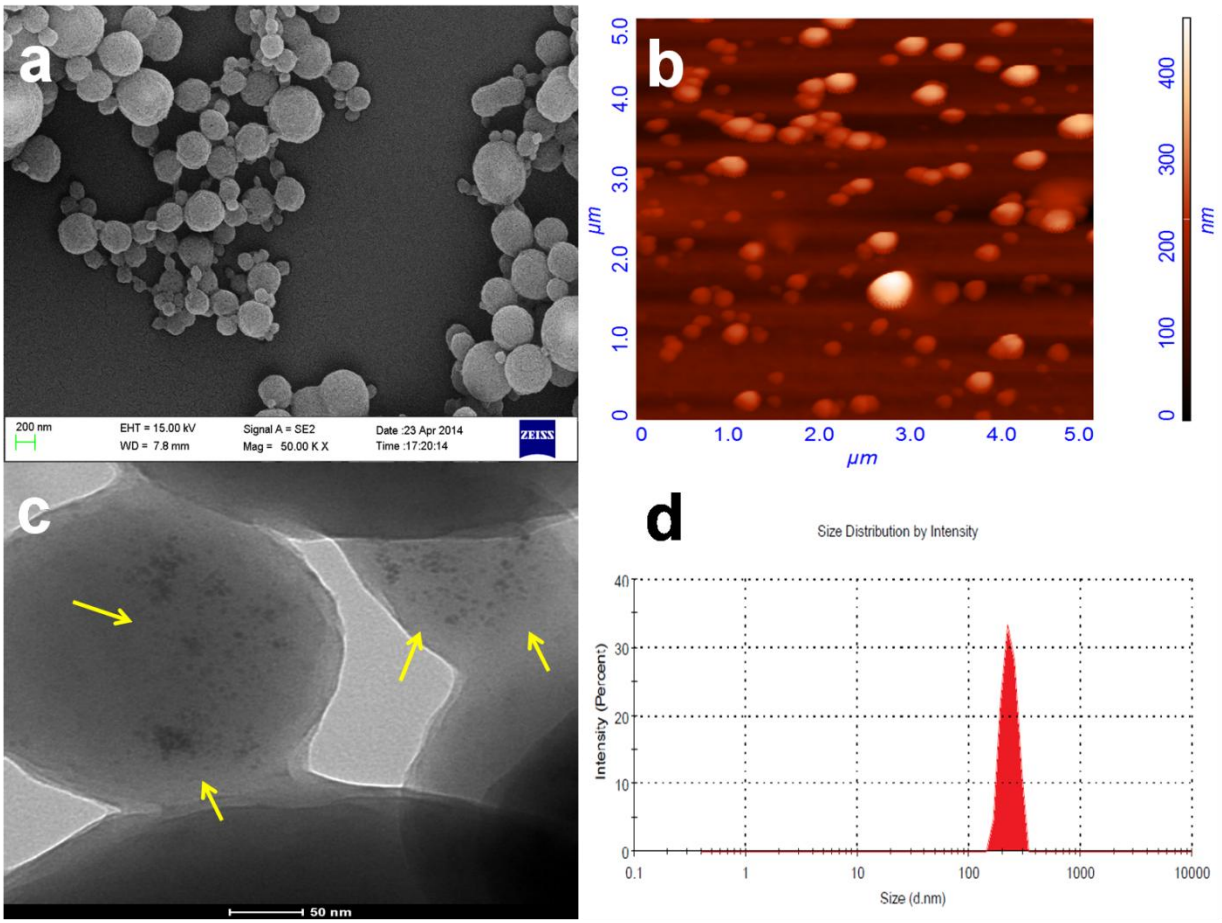

Fig.2 (a) FE-SEM and (b) AFM images of BCNPs showing their typical morphology (c) TEM image of BCNPs showing the encapsulated CNPs (indicated by yellow arrows) and (d) DLS image of BCNPs showing the distribution and size of nanoparticles.

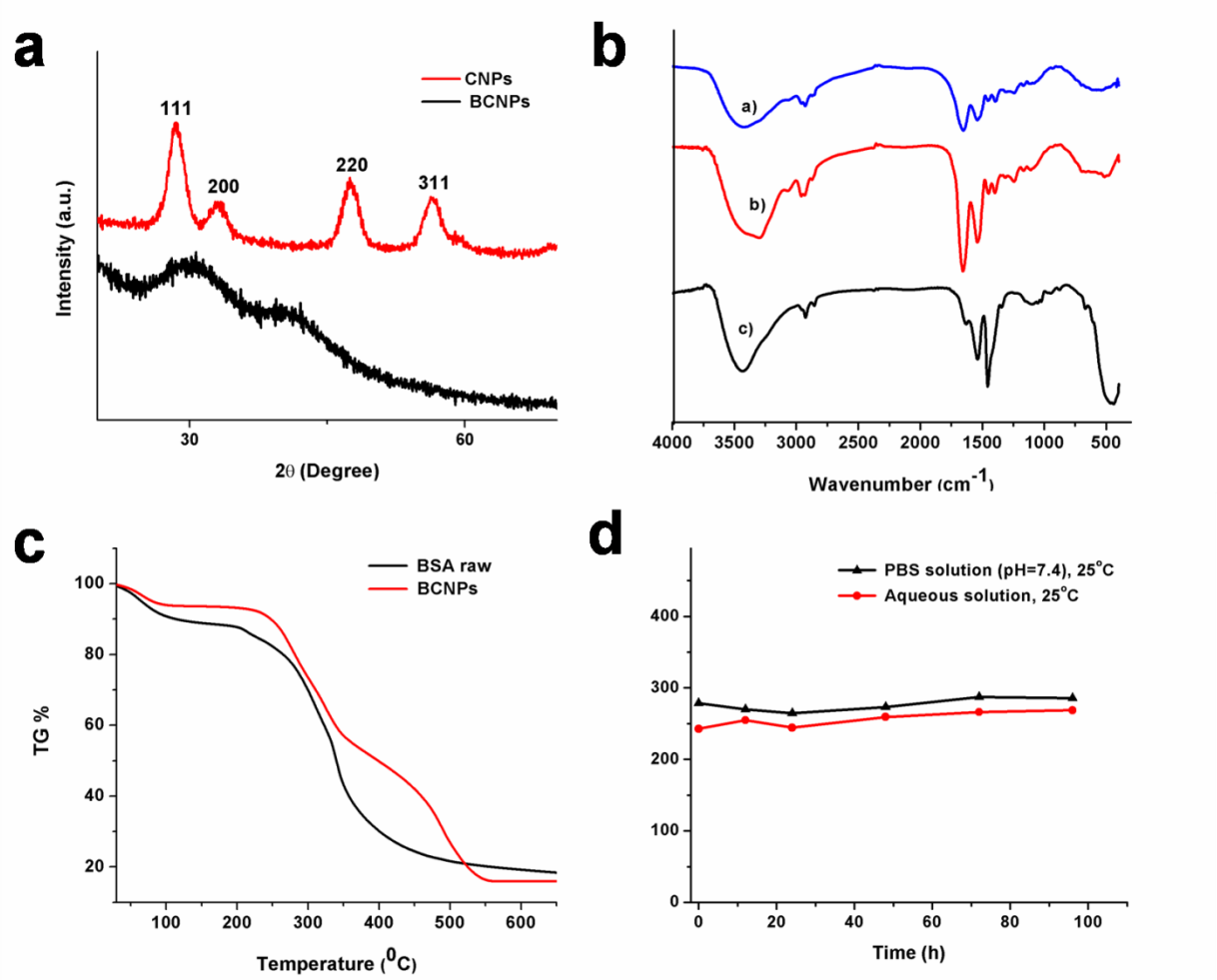

Fig.3 (a) XRD plot of CNPs and BCNPs (b) FTIR spectra of BSA (control), CNPs and BCNPs (c) TG data curve of BSA (control) and BCNPs (d) *In vitro* stability of BCNPs in aqueous and PBS (pH =7.4) solutions.

a

Protein Concentration (mg)	CNPs concentration (mg)	Entrapment efficiency (%)
25	1	67.70±1.155
25	3	74.80±2.413
25	5	82.34±1.481
25	10	76.81±2.478

b

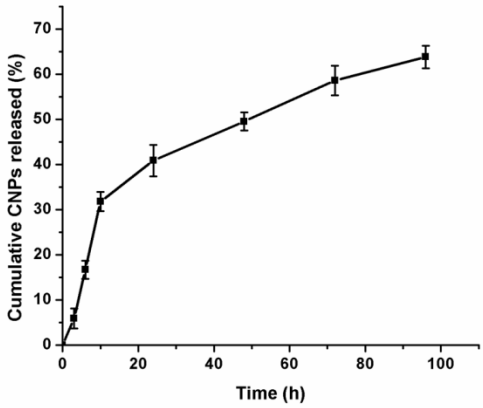

Fig. 4 (a) Entrapment efficiency of BCNPs with varying CNPs concentrations (b) CNPs release profile from BCNPs in PBS.

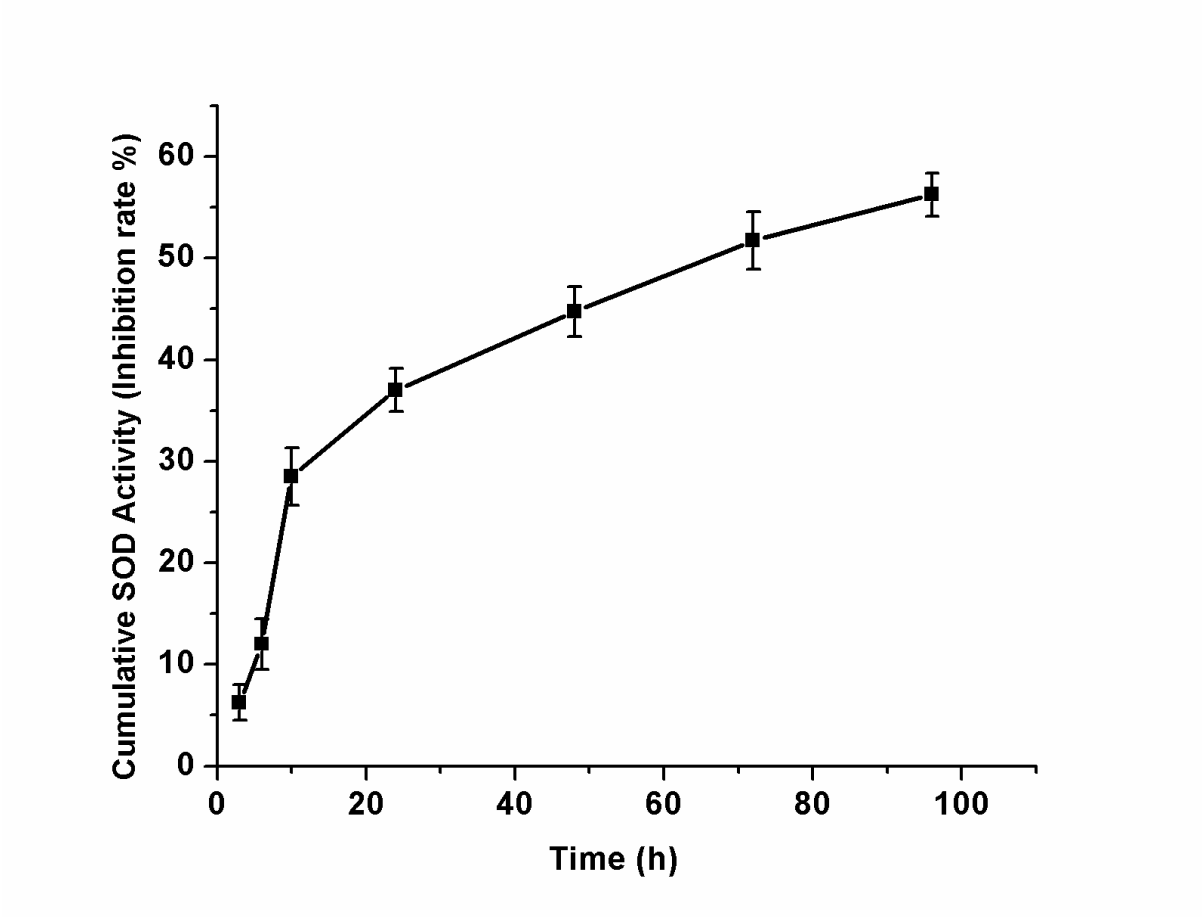

Fig. 5 SOD activity (inhibition rate %) of the released CNPs from BCNPs showing the increase in SOD activity as a function of time.

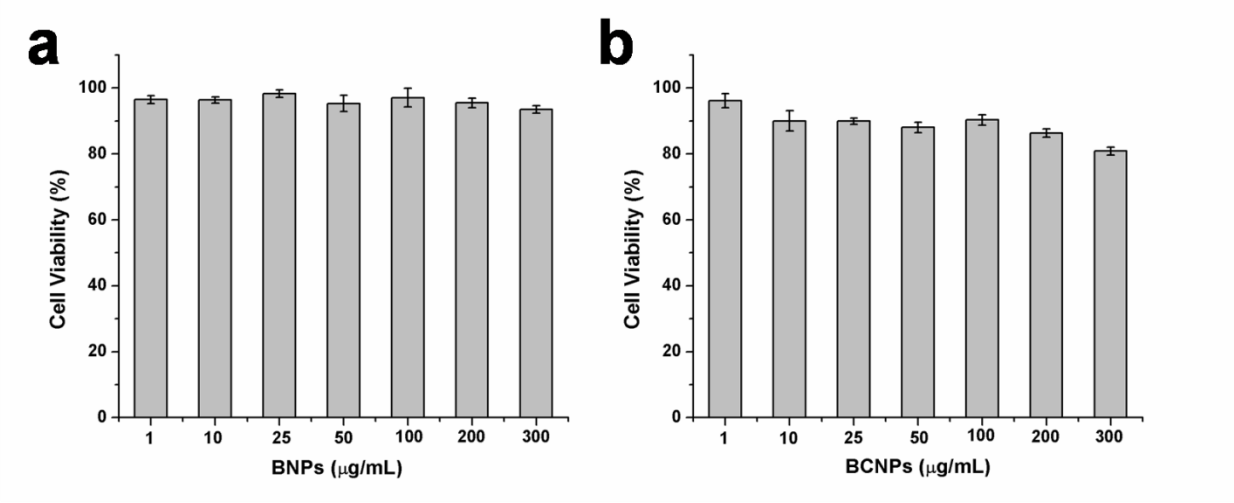

Fig. 6 Biocompatibility and cell viability assay (MTT assay) of (a) BNPs and (b) BCNPs on L-132 cells.

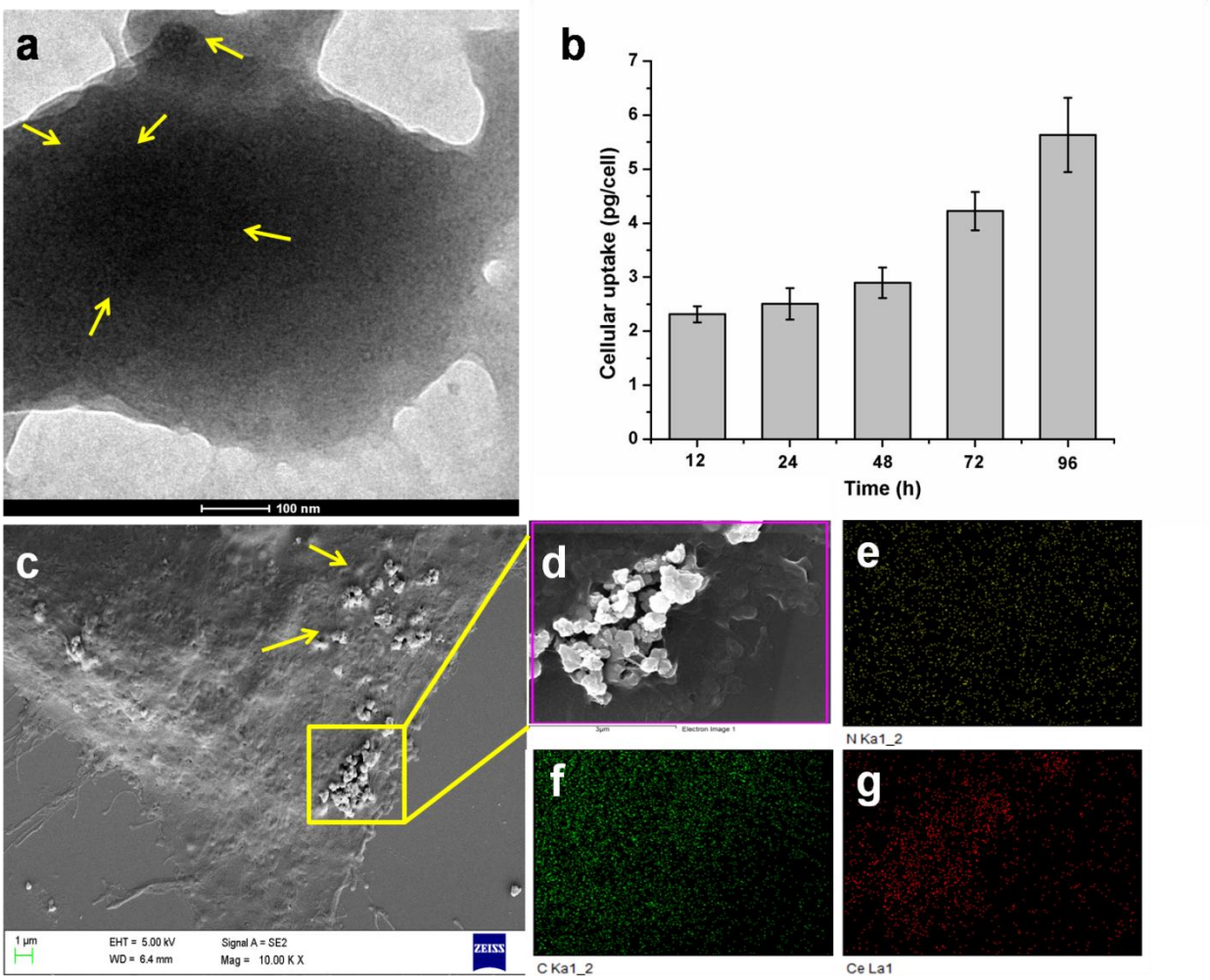

Fig. 7 (a) TEM image of L-132 cells with internalized BCNPs indicated by yellow arrow (b) Quantification of BCNPs internalized by L-132 cells with increase in preincubation time. (c) Representative FE-SEM image of L-132 cells with BCNPs, arrows indicates the BCNPs attached on the surface of cell. (d) Magnified FE-SEM image of L-132 cell with internalized BCNPs and (e-f) color coded SEM/EDX dot maps depicting the individual elemental distribution. (Yellow for nitrogen, green for carbon and red for cerium). The scale bars in (a) 100 nm and (c) 1 µm.

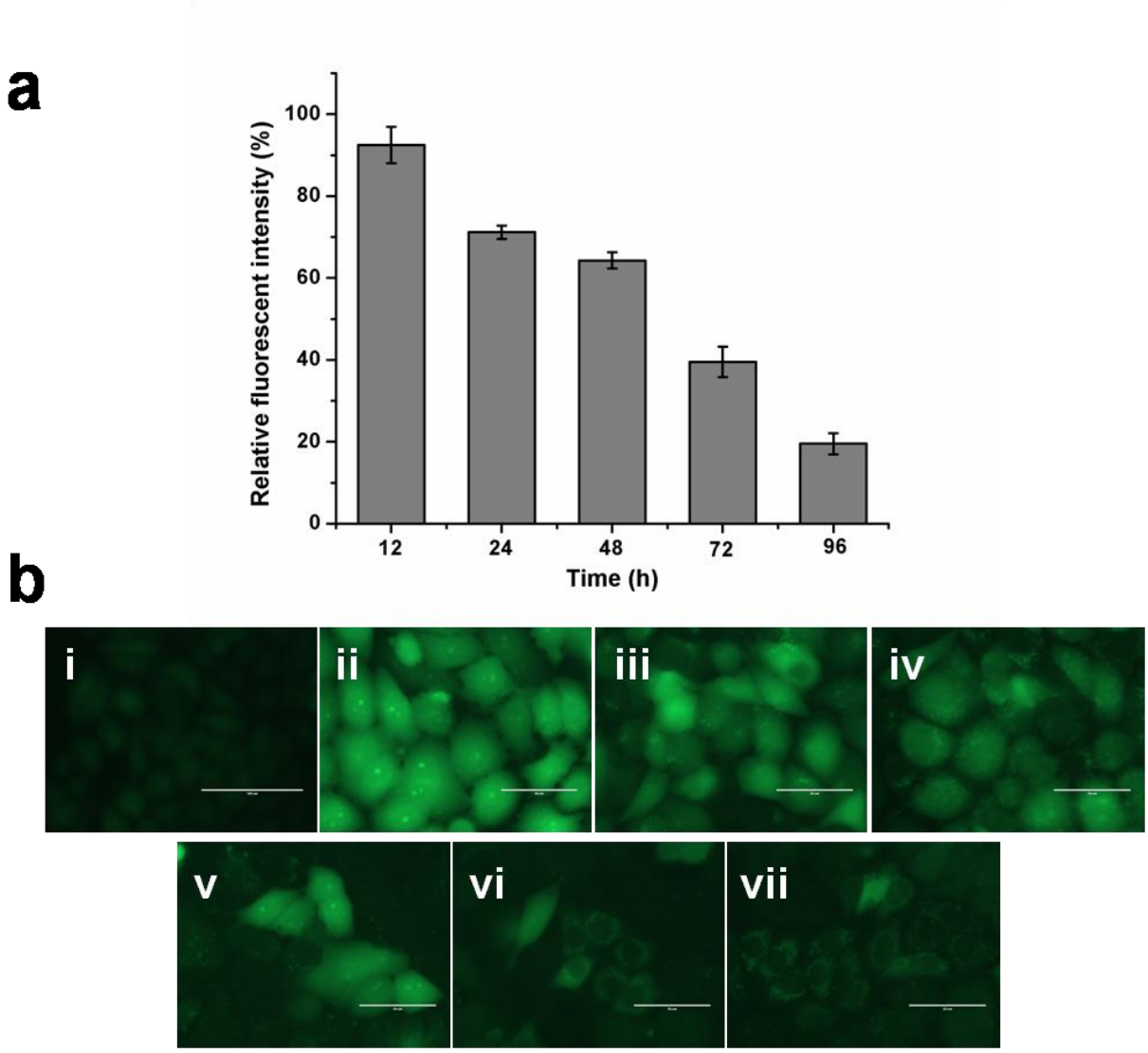

Fig. 8 (a) Scavenging of ROS by BCNPs in L-132 cells. (b) Representative florescence images of H_2O_2-treated L-132 cells after staining with DCFH-DA. (i) Untreated cells (ii) H_2O_2 treated cells without BCNPs preincubation and (iii-vii) H_2O_2 treated cells with increase in BCNPs preincubation time. All the scale bars represent 50 μm.

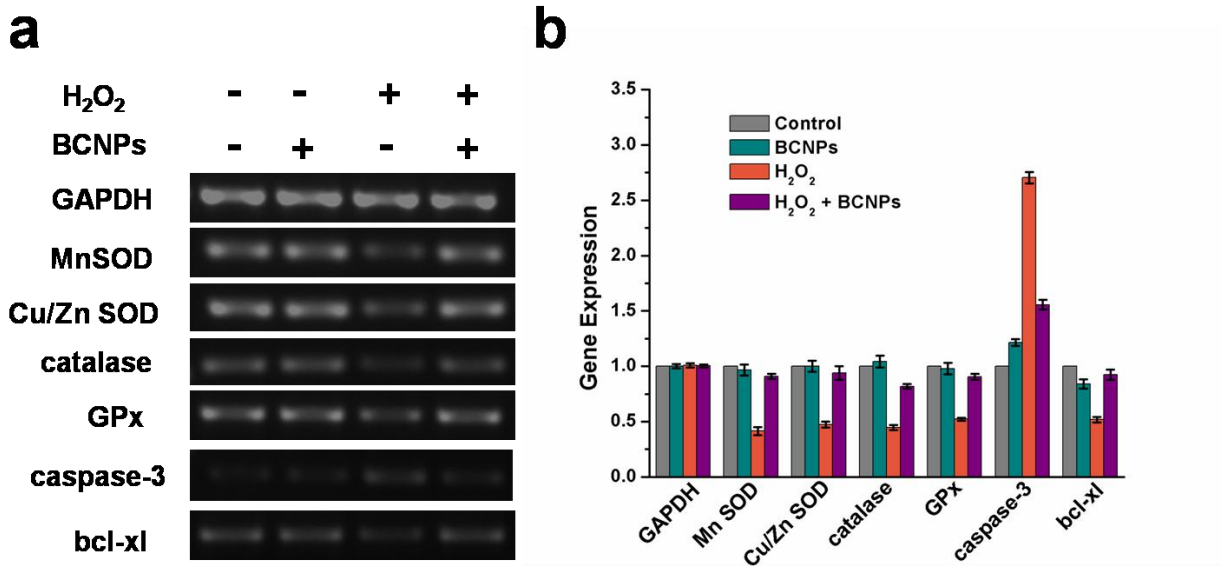

Fig. 9 (a) Semi-quantitative RT-PCR analysis of antioxidant and apoptotic genes. (b) Fold difference in gene expression in treated L-132 cells compared to untreated L-132 cells.

Graphical abstract